



Article

# Spatial Distribution and Health Risk Assessment of Potentially Toxic Elements in Surface Soils of Bosten Lake Basin, Central Asia

Long Ma <sup>1,2,3,\*</sup> , Jilili Abuduwaili <sup>1,2,3</sup> and Wen Liu <sup>1,2,3</sup>

<sup>1</sup> State Key Laboratory of Desert and Oasis Ecology, Xinjiang Institute of Ecology and Geography, Chinese Academy of Sciences, Urumqi 830011, China; Jilil@ms.xjb.ac.cn (J.A.); liuwen@ms.xjb.ac.cn (W.L.)

<sup>2</sup> Research Center for Ecology and Environment of Central Asia, Chinese Academy of Sciences, Urumqi 830011, China

<sup>3</sup> University of Chinese Academy of Sciences, Beijing 10049, China

\* Correspondence: malong@ms.xjb.ac.cn

Received: 22 August 2019; Accepted: 1 October 2019; Published: 4 October 2019



**Abstract:** A geographically weighted regression and classical linear model were applied to quantitatively reveal the factors influencing the spatial distribution of potentially toxic elements of forty-eight surface soils from Bosten Lake basin in Central Asia. At the basin scale, the spatial distribution of the majority of potentially toxic elements, including: cobalt (Co), chromium (Cr), copper (Cu), nickel (Ni), lead (Pb), thallium (Tl), vanadium (V), and zinc (Zn), had been significantly influenced by the geochemical characteristics of the soil parent material. However, the arsenic (As), cadmium (Cd), antimony (Sb), and mercury (Hg) have been influenced by the total organic matter in soils. Compared with the results of the classical linear model, the geographically weighted regression can significantly increase the level of simulation at the basin spatial scale. The fitting coefficients of the predicted values and the actual measured values significantly increased from the classical linear model (Hg:  $r^2 = 0.31$ ; Sb:  $r^2 = 0.64$ ; Cd:  $r^2 = 0.81$ ; and As:  $r^2 = 0.68$ ) to the geographically weighted regression (Hg:  $r^2 = 0.56$ ; Sb:  $r^2 = 0.74$ ; Cd:  $r^2 = 0.89$ ; and As:  $r^2 = 0.85$ ). Based on the results of the geographically weighted regression, the average values of the total organic matter for As (28.7%), Cd (39.2%), Hg (46.5%), and Sb (26.6%) were higher than those for the other potentially toxic elements: Cr (0.1%), Co (4.0%), Ni (5.3%), V (0.7%), Cu (18.0%), Pb (7.8%), Tl (14.4%), and Zn (21.4%). There were no significant non-carcinogenic risks to human health, however, the results suggested that the spatial distribution of potentially toxic elements had significant differences.

**Keywords:** arid land; classical linear model; geographically weighted regression; influencing factors; soil geochemistry

## 1. Introduction

The influence of human activities on the surface of the Earth has continued to increase over the past hundred years [1–3]. Trace elements in surface agricultural soils are easily influenced by human activities via atmospheric deposition, irrigation, and fertilizer usage [4,5]. Long-term inputs of potentially toxic elements will lead to the enrichment of ecosystems and will be increasingly toxic to organisms [6–8]. It is not surprising that soil research has increased exponentially in recent decades [9,10]. However, it is undeniable that previous research areas have been mainly concentrated in developed regions [11–13].

From the aspect of the research methods used for pollution of potentially toxic elements, classic statistical methods have been used to reveal the possible influencing factors [14–16]. However, many researchers have given more consideration to influences on the distribution of potentially toxic elements

from a quantitative point of view [17–20]. The geographical setting and climatic conditions of Central Asia led to ecological fragility and low carrying capacity in this region [21]. Research often focuses on the influence of human activities on land use and land cover changes [22,23], and soil degradation in Central Asia [24–27]. However, studies on potentially toxic elements in soils in this region have been scarce [28]. By studying the current risk state of potentially toxic elements in soils in this typical region, we can obtain a better understanding of the distribution of potentially toxic elements with different influential factors in Central Asia. The results will reveal the potentially toxic elements that are susceptible to human activities and will provide significant information for resource protection and management in the future.

The Bosten Lake region has begun to experience large-scale development. Due to the importance of the Bosten Lake region, studies on the paleoclimatic [29] and paleoenvironmental evolution [30] of the region and the pollution caused by polycyclic aromatic hydrocarbons [31,32], heavy metals [33,34], and organochlorine pesticides [35] have been performed for Bosten Lake sediments. In this study, using classic statistical methods and geographically weighted regression modeling [36–39], the influencing factors of potentially toxic elements in surface soils in this region, combined with a quantitative method and the assessment of the pollution of potentially toxic elements, are revealed in a typical arid area (Bosten Lake region) in Central Asia.

## 2. Materials and Methods

### 2.1. Regional Settings

The Bosten Lake basin lies between the Tian Shan Mountains and the Taklamakan Desert (Figure 1) and has a typical arid climate [40]. To the north is Aragou Mountain (Mt.) with a peak of 4000–4300 m above sea level. Hora Mt. and Kuruktag Mt. are to the south with elevations of 3000–2000 m. Erbin Mt. is to the west with an elevation greater than 4300 m. There are dry hills to the east at altitudes below 2000 m. In the 1960s, the farmland area was 1174.86 km<sup>2</sup> and by the early 1990s, the area increased by 760.41 km<sup>2</sup> [41]. The total annual precipitation is only 76.1 mm; however, evaporation amounts to 2000 mm year<sup>-1</sup> [42]. There are four counties, including Yanqi, Hejing, Heshuo, and Bohu, in the Bosten Lake region. Over the past half-century, the economy has developed rapidly. We calculated the sums of several economic variables, including the year-end population, gross domestic product (GDP), total sown area for farm crops, and the number of industrial enterprises, to confirm the rapid growth in the region. For example, the GDP sharply increased from  $5.6 \times 10^6$  Chinese Yuan (CNY) in 1949 to  $3.8 \times 10^8$  CNY in 2004, which reflected the dramatic increase in human activities.

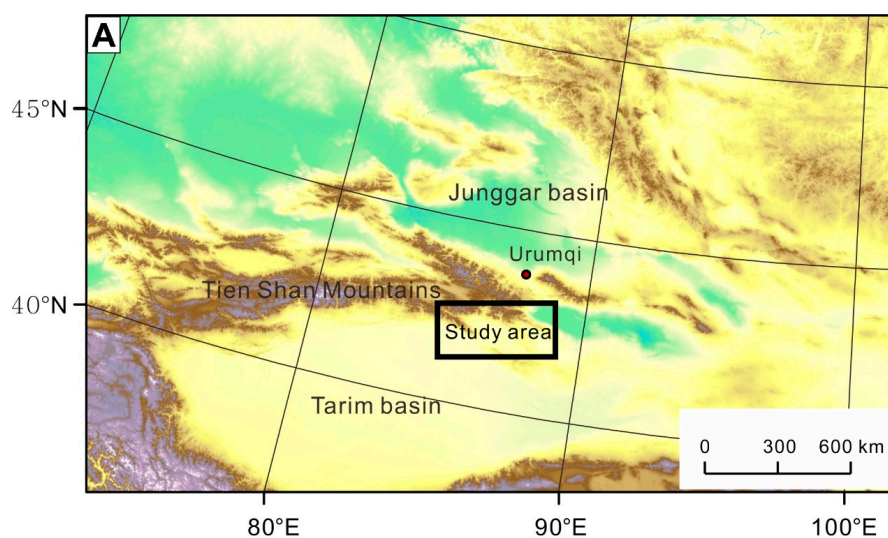
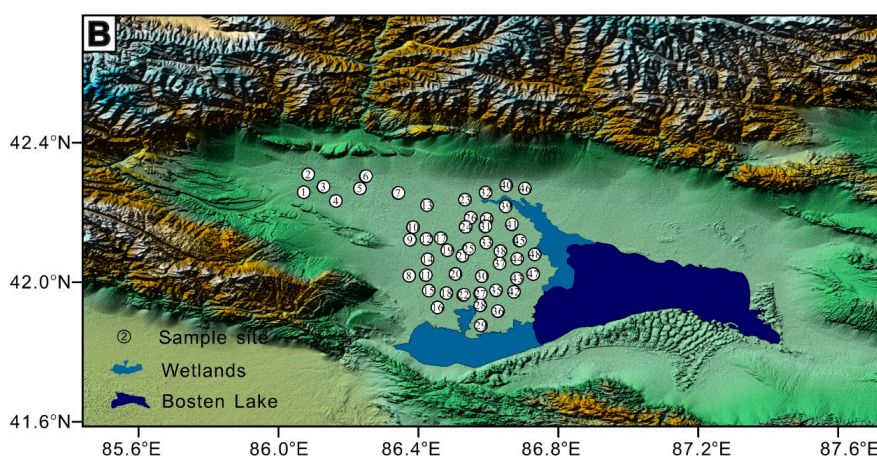


Figure 1. Cont.



**Figure 1.** The geographical location of the Bosten Lake region (A) and the sampling sites (B).

In addition, Bosten Lake is a basin that was previously the largest inland freshwater lake in China, with a water surface area greater than 1000 km<sup>2</sup> [43]. Because various basin materials are not exported from the basin and are instead discharged into lakes, Bosten Lake has undergone significant changes under the pressure of human activities, for example, the salinity has increased from 0.38 to 1.87 g L<sup>-1</sup> [44]. Changes in the geochemical composition of surface soils in the basin directly control the materials, ecosystem structure, and ecological security of Bosten Lake.

## 2.2. Sampling and Analyses

Surface soil samples (0–5 cm) were collected at 48 sampling sites in the Bosten Lake basin (Figure 1). At each sampling site, the soil sample was mixed with 5 sub-samples that were distributed at the center and four points of a 2 m × 2 m square with a sampling style of “×” form. The content of total organic matter (TOM) was confirmed via oxidation by using the potassium dichromate method [45]. Bulk soils with masses of ~0.125 g were ground through a 200-μm size mesh, digested with HF–HNO<sub>3</sub>–HClO<sub>4</sub>, and analysed using inductively coupled plasma atomic emission spectroscopy for the elements (Fe and V) and inductively coupled plasma mass spectrometry for the potentially toxic elements: As, Cd, Co, Cr, Cu, Hg, Ni, Pb, Sb, Tl, and Zn.

## 2.3. Data Analyzing

A principal component analysis potentially assisted in identifying the probable factors influencing the distribution patterns of pollution [46–48]. Pearson correlation analysis [49] was used to reveal the inter-relationships among the Fe and the potentially toxic elements (As, Cd, Co, Cr, Cu, Hg, Ni, Pb, Sb, Tl, and Zn). Kolmogorov–Smirnov (K–S) test was also applied to conduct normality tests.

A classical linear model assumes that the estimated coefficient for the independent variable is constant [50]. The model presumes that the value of Y has a linear correlation with a set of environmental variables ( $X_i$ ) as follows:

$$y = \beta_0 + \sum_{i=1}^n \beta_i x_i \quad (1)$$

In contrast, geographically weighted regression is a traditional method that extracts a set of local parameters [51,52] and shows a relationship that varies in space, which can be written as:

$$y_j = \beta_0(u_j, v_j) + \sum_{i=1}^p \beta_i(u_j, v_j) x_{ij} \quad (2)$$

where  $u_j, v_j$  represents the coordinates for each location  $j$ ,  $\beta_0(u_j, v_j)$  represents the intercept, and  $\beta_i(u_j, v_j)$  is a local parameter for variable  $X_i$  at location  $j$ . Details on the geographically weighted regression can be found in the user manual for GWR4 software package version 4.09 [53]. To evaluate the modeling results, the parameters, including the Nash–Sutcliffe efficiency (NSE), percentage bias (PBIAS), and root mean square error (RSE), were calculated as follows [54]:

$$\text{NSE} = 1 - \frac{\sum_{i=1}^n (X_i - \hat{X}_i)^2}{\sum_{i=1}^n (X_i - \bar{X})^2} \quad (3)$$

$$\text{RSR} = \frac{\sqrt{\sum_{i=1}^n (X_i - \hat{X}_i)^2}}{\sqrt{\sum_{i=1}^n (X_i - \bar{X})^2}} \quad (4)$$

$$\text{PBIAS} = \frac{\sum_{i=1}^n (X_i - \hat{X}_i) \times 100}{\sum_{i=1}^n X_i} \quad (5)$$

where  $X_i, \hat{X}_i, \bar{X}$ , and  $n$  represents the actual monitoring value, the modeled value, the average value of the actual monitoring value, and the number of monitoring samples, respectively.

Developed by the United States Environmental Protection Agency, human health risk assessment was used to calculate a non-carcinogenic hazards index for adult exposure to potentially toxic elements.

$\text{ADD}_{\text{ing}}$  represents the average daily intake via ingestion:

$$\text{ADD}_{\text{ing}}(\text{mg} \cdot \text{kg}^{-1} \cdot \text{day}^{-1}) = C \times \frac{\text{IngR} \times \text{EF} \times \text{ED}}{\text{BW} \times \text{AT}} \times 10^{-6} \quad (6)$$

where  $C$  represents the potentially toxic element content ( $\text{mg kg}^{-1}$ ), and the maximum value of the potentially toxic elements was used to calculate the non-carcinogenic risk.  $\text{IngR}$  represents the ingestion rate ( $200 \text{ mg day}^{-1}$ ) [55],  $\text{EF}$  represents the exposure frequency ( $350 \text{ day year}^{-1}$ ) [56],  $\text{ED}$  represents the exposure duration (30 years) [56],  $\text{BW}$  represents the body weight (70 kg) [56], and  $\text{AT}$  represents the exposure time ( $\text{AT} = 365 \times \text{ED}$ ).

$\text{ADD}_{\text{inh}}$  represents the average daily intake via inhalation:

$$\text{ADD}_{\text{inh}}(\text{mg} \cdot \text{kg}^{-1} \cdot \text{day}^{-1}) = C \times \frac{\text{InhR} \times \text{EF} \times \text{ED}}{\text{PEF} \times \text{BW} \times \text{AT}} \quad (7)$$

where  $\text{InhR}$  represents the inhalation rate ( $12.8 \text{ m}^3 \text{ day}^{-1}$ ) [57] and  $\text{PEF}$  is the particle emission factor ( $1.36 \times 10^9 \text{ m}^3 \text{ kg}^{-1}$ ) [55].

$\text{ADD}_{\text{derm}}$  represents the average daily intake via dermal absorption:

$$\text{ADD}_{\text{derm}}(\text{mg} \cdot \text{kg}^{-1} \cdot \text{day}^{-1}) = C \times \frac{\text{SA} \times \text{SL} \times \text{ABS} \times \text{EF} \times \text{ED}}{\text{BW} \times \text{AT}} \times 10^{-6} \quad (8)$$

where  $\text{SA}$  represents the exposed skin area ( $4350 \text{ cm}^2$ ) [57],  $\text{SL}$  is the skin adherence factor ( $0.2 \text{ mg cm}^{-2} \text{ day}^{-1}$ ) [55], and  $\text{ABS}$  represents the dermal absorption factor (dimensionless,  $\text{ABS} = 0.001$ ). For  $\text{As}$ ,  $\text{ABS} = 0.03$  [55].

For exposure pathway  $i$ , non-carcinogenic hazards, such as a hazard quotient (HQ), are calculated with the rate of the corresponding reference dose for exposure pathway  $i$  ( $RfD_i$ ):

$$HQ_i = ADD_i/RfD_i \quad (9)$$

The hazard index (HI) is calculated as follows:

$$HI = \sum_{i=1}^3 HQ_i \quad (10)$$

If  $HI < 1$  or  $HQ < 1$ , it is suggested that there are no non-carcinogenic risks. If  $HI > 1$  or  $HQ > 1$ , it is inferred that non-carcinogenic effects occurred [58].

### 3. Results and Discussions

#### 3.1. Basic Statistical Results for the Contents of Major Elements and Potentially Toxic Elements

The contents for TOM and soil elements, including iron (Fe), arsenic (As), cadmium (Cd), cobalt (Co), chromium (Cr), copper (Cu), nickel (Ni), lead (Pb), antimony (Sb), thallium (Tl), vanadium (V), and zinc (Zn), and the health risk assessment for potentially toxic elements are shown in Table 1. The average content of Fe is  $27.07 \text{ g kg}^{-1}$ , and the average value of TOM is  $14.59 \text{ g kg}^{-1}$  (Table 1). Among the potentially toxic elements, Hg, Cd, Sb, and Tl have the lowest average contents. In the Bosten Lake basin, the concentrations of TOM and soil elements are normally distributed ( $p > 0.05$ ).

**Table 1.** Descriptive statistical analysis of major elements and potentially toxic elements in the surface soils of the Bosten Lake basin.

| Composition      | Unit                | LOD <sup>b</sup> | Basic Statistics |         |         |                    |                |
|------------------|---------------------|------------------|------------------|---------|---------|--------------------|----------------|
|                  |                     |                  | Minimum          | Maximum | Average | Standard Deviation | Standard Error |
| TOM <sup>a</sup> | $\text{g kg}^{-1}$  | 0.01             | 4.46             | 23.43   | 14.59   | 5.17               | 0.75           |
| Fe               | $\text{g kg}^{-1}$  | 0.005            | 19.50            | 35.50   | 27.07   | 3.50               | 0.51           |
| V                | $\text{mg kg}^{-1}$ | 2                | 54.50            | 94.18   | 72.83   | 9.09               | 1.31           |
| Zn               | $\text{mg kg}^{-1}$ | 0.1              | 28.30            | 85.80   | 58.00   | 13.71              | 1.98           |
| Cr               | $\text{mg kg}^{-1}$ | 0.1              | 32.27            | 74.05   | 49.60   | 8.69               | 1.25           |
| Co               | $\text{mg kg}^{-1}$ | 0.01             | 5.46             | 12.84   | 8.92    | 1.62               | 0.23           |
| Ni               | $\text{mg kg}^{-1}$ | 0.05             | 12.53            | 35.40   | 23.09   | 4.75               | 0.69           |
| Cu               | $\text{mg kg}^{-1}$ | 0.02             | 5.46             | 28.94   | 17.94   | 5.20               | 0.75           |
| As               | $\text{mg kg}^{-1}$ | 0.1              | 5.30             | 13.67   | 9.86    | 2.02               | 0.29           |
| Cd               | $\text{mg kg}^{-1}$ | 0.01             | 0.09             | 0.20    | 0.15    | 0.03               | 0.00           |
| Sb               | $\text{mg kg}^{-1}$ | 0.05             | 0.68             | 1.47    | 1.05    | 0.20               | 0.03           |
| Tl               | $\text{mg kg}^{-1}$ | 0.02             | 0.34             | 0.58    | 0.44    | 0.05               | 0.01           |
| Pb               | $\text{mg kg}^{-1}$ | 0.01             | 13.95            | 21.93   | 17.05   | 1.71               | 0.25           |
| Hg               | $\text{ng g}^{-1}$  | 0.01             | 10.75            | 31.00   | 20.62   | 4.67               | 0.67           |

<sup>a</sup>: The content of total organic matter; <sup>b</sup>: Limit of detection.

#### 3.2. Influencing Factors for the Variation of Potentially Toxic Elements

A principal component analysis was used to analyze the potential influencing factors for the variation of potentially toxic elements. Two components were extracted, which accounted for 89.2% of the total variance in the data set for potentially toxic elements (Table S1, supplementary electronic files). The potentially toxic elements were grouped according to their loadings (Figure 2). The first component accounted for 57.5% and formed a group composed of V, Ni, Cr, Co, Zn, Cu, Pb, and Tl, which had high loadings of V (0.91), Ni (0.95), Cr (0.95), Co (0.93), Zn (0.83), Cu (0.83), Pb (0.76), and Tl (0.81). The second component accounted for 31.7% and formed another group composed of Hg, Sb, Cd,

and As, which had high loadings of Hg (0.86), Sb (0.77), Cd (0.76), and As (0.78) (Figure 2). Through principal component analysis, it is concluded that there are obvious differences in the influencing factors between the two groups of potentially toxic elements.

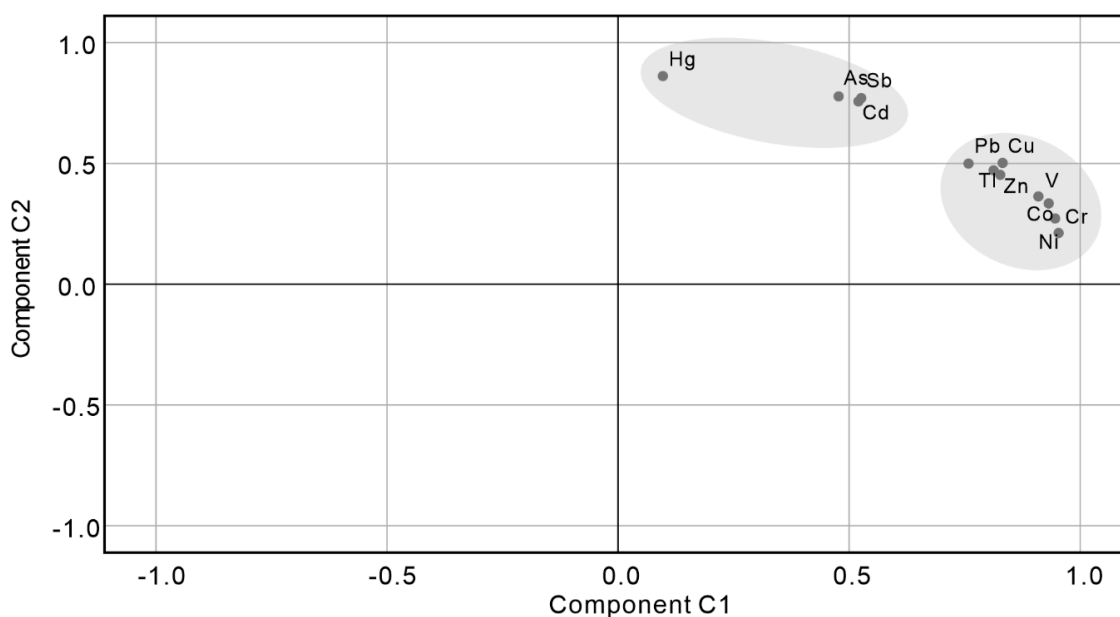


**Figure 2.** The component-loading plot of the potentially toxic elements, which indicates the potential influencing factors.

Fe is always used as a reference element for parent materials to calculate the enrichment of potentially toxic elements [59,60]. At a small scale, the background concentration gradients of the elements can be assumed to be uniform [61]. Coefficient of determinations for linear fitting were calculated among Fe and the potentially toxic elements (V:  $r^2 = 0.95$ ; Cr:  $r^2 = 0.96$ ; Co:  $r^2 = 0.96$ ; Ni:  $r^2 = 0.93$ ; Cu:  $r^2 = 0.81$ ; Pb:  $r^2 = 0.73$ ; Tl:  $r^2 = 0.73$ ; Zn:  $r^2 = 0.70$ ; As:  $r^2 = 0.46$ ; Cd:  $r^2 = 0.47$ ; Sb:  $r^2 = 0.49$ ; and Hg:  $r^2 = 0.17$ ) (Figure 3). The Pearson correlation coefficients with two-tailed significance tests were also calculated to reveal the inter-relationships among the Fe and the potentially toxic elements (V:  $r = 0.979$ ,  $p < 0.001$ ; Cr:  $r = 0.979$ ,  $p < 0.001$ ; Co:  $r = 0.982$ ,  $p < 0.001$ ; Ni:  $r = 0.965$ ,  $p < 0.001$ ; Cu:  $r = 0.903$ ,  $p < 0.001$ ; Pb:  $r = 0.857$ ,  $p < 0.001$ ; Tl:  $r = 0.867$ ,  $p < 0.001$ ; Zn:  $r = 0.850$ ,  $p < 0.001$ ; As:  $r = 0.692$ ,  $p < 0.001$ ; Cd:  $r = 0.719$ ,  $p < 0.001$ ; Sb:  $r = 0.710$ ,  $p < 0.001$ ; and Hg:  $r = 0.425$ ,  $p = 0.0017$ ). Notably, the contents of potentially toxic elements (Hg, Sb, Cd, and As) showed a relatively weaker correlation with Fe, and many samples showed a deviation during the simple linear regression, indicating that some potential influencing factor (e.g., TOM) other than the soil parent materials, had some impact on these four potentially toxic elements.

To quantitatively analyse the relationships among the potentially toxic elements, Fe, and TOM in the soils, the potentially toxic elements (Hg, Sb, Cd, and As) were assigned as the dependent variable, and Fe and TOM were chosen as the independent variables in the models of the geographically weighted regression and the classical linear model. When modelling with the classical linear model (Figure 4), the fitting coefficients for the predicted values and actual measured values were found (Hg:  $r^2 = 0.31$ ; Sb:  $r^2 = 0.64$ ; Cd:  $r^2 = 0.81$ ; and As:  $r^2 = 0.68$ ). Due to the results of the geographically weighted regression, the correlation coefficients significantly improved (Hg:  $r^2 = 0.56$ ; Sb:  $r^2 = 0.74$ ; Cd:  $r^2 = 0.89$ ; and As:  $r^2 = 0.85$ ). Combined with the evaluation of the modeling results, which was based on the evaluation criterion, the results via the geographically weighted regression were acceptable (Table 2). The residuals from the results of the geographically weighted regression and classical linear model passed the normality test (Figure S1, supplementary electronic files). From a geographic perspective, the relationships among the potentially toxic elements, Fe and TOM had

geographical or spatial heterogeneity, and the uniform values generated by the classical statistics ignored the geographical control on the distributions of potentially toxic elements.

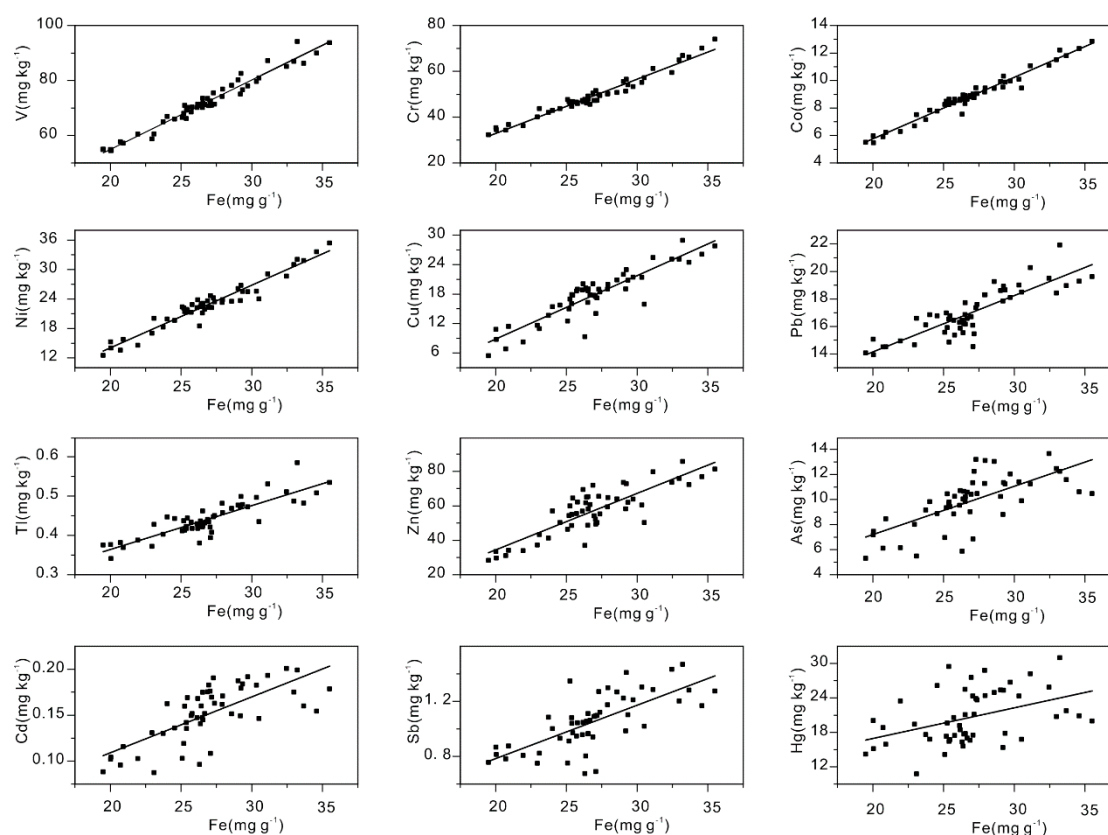


**Figure 3.** Scatter plots showing the potentially toxic elements (V, Cr, Co, Ni, Cu, Pb, Tl, Zn, As, Cd, Hg, and Sb) versus the content of Fe via a linear regression.

**Table 2.** General performance ratings for the results of the geographically weighted regression and multiple classical linear models for potentially toxic elements (PTEs).

| PTEs            | Model Equation  | RSE <sup>c</sup> | NSE <sup>d</sup> | PBIAS <sup>e</sup> | Performance Rating <sup>f</sup> |
|-----------------|---|------------------|------------------|--------------------|---------------------------------|
| As <sup>a</sup> | $[As] = 2.04 \times 10^{-1} \times [Fe] + 2.23 \times 10^{-1} \times [TOM] + 1.10$                | 0.57             | 0.68             | 0.00               | Good                            |
| Cd <sup>a</sup> | $[Cd] = 2.42 \times 10^{-3} \times [Fe] + 4.15 \times 10^{-3} \times [TOM] + 2.56 \times 10^{-2}$ | 0.44             | 0.81             | -0.10              | Very good                       |
| Sb <sup>a</sup> | $[Sb] = 2.39 \times 10^{-2} \times [Fe] + 1.85 \times 10^{-2} \times [TOM] + 1.36 \times 10^{-1}$ | 0.60             | 0.64             | -0.001             | Satisfactory                    |
| Hg <sup>a</sup> | $[Hg] = 1.85 \times 10^{-1} \times [Fe] + 4.23 \times 10^{-1} \times [TOM] + 9.45$                | 0.83             | 0.31             | 0.00               | Unsatisfactory                  |
| As <sup>b</sup> | $[As]^e = [\beta_1]_{As} \times [Fe] + [\beta_2]_{As} \times [TOM] + [\beta_0]_{As}$              | 0.39             | 0.85             | 0.03               | Very good                       |
| Cd <sup>b</sup> | $[Cd]^e = [\beta_1]_{Cd} \times [Fe] + [\beta_2]_{Cd} \times [TOM] + [\beta_0]_{Cd}$              | 0.34             | 0.88             | 0.13               | Very good                       |
| Sb <sup>b</sup> | $[Sb]^e = [\beta_1]_{Sb} \times [Fe] + [\beta_2]_{Sb} \times [TOM] + [\beta_0]_{Sb}$              | 0.51             | 0.74             | -0.20              | Good                            |
| Hg <sup>b</sup> | $[Hg]^e = [\beta_1]_{Hg} \times [Fe] + [\beta_2]_{Hg} \times [TOM] + [\beta_0]_{Hg}$              | 0.68             | 0.54             | -0.36              | Satisfactory                    |

<sup>a</sup>: Classical linear model; <sup>b</sup>: Geographically weighted regression, the detailed parameters are shown in Table S2 (supplementary electronic files); <sup>c</sup>: Root mean square error; <sup>d</sup>: Nash–Sutcliffe efficiency; <sup>e</sup>: Percentage bias; <sup>f</sup>: Performance ratings followed common criteria of the reference [54].

Based on the acceptance and validity of the geographically weighted regression, all of the potentially toxic elements As, Cd, Co, Cr, Cu, Ni, Pb, Sb, Tl, V, and Zn were simulated. By calculating the ratio of the part of the potentially toxic elements affected by the organic matter content, we can see that potentially toxic elements such as As, Cd, Hg, and Sb have average values of 28.8%, 39.2%, 46.5%, and 26.6% for the contents influenced by organic matter, respectively (Figure 5). The contents of potentially toxic elements are relatively low in soils, and changes in environmental conditions (e.g., climate, type, duration, and intensity of human activity) can easily have a profound impact on the

distribution and content of elements. The main irrigation method in the oasis of this basin is drip irrigation. Existing studies have shown that fertilizers contain potentially toxic elements, such as Zn, Cu, Pb, Cd, As, and Hg [62–64], and a large amount of water-soluble fertilizer enters the soil via drip irrigation. Notably, the source of the influence of the organic matter has not yet been identified in this article. The potentially toxic elements affected by organic matter may come from human activities or from the process of soil formation under natural conditions.

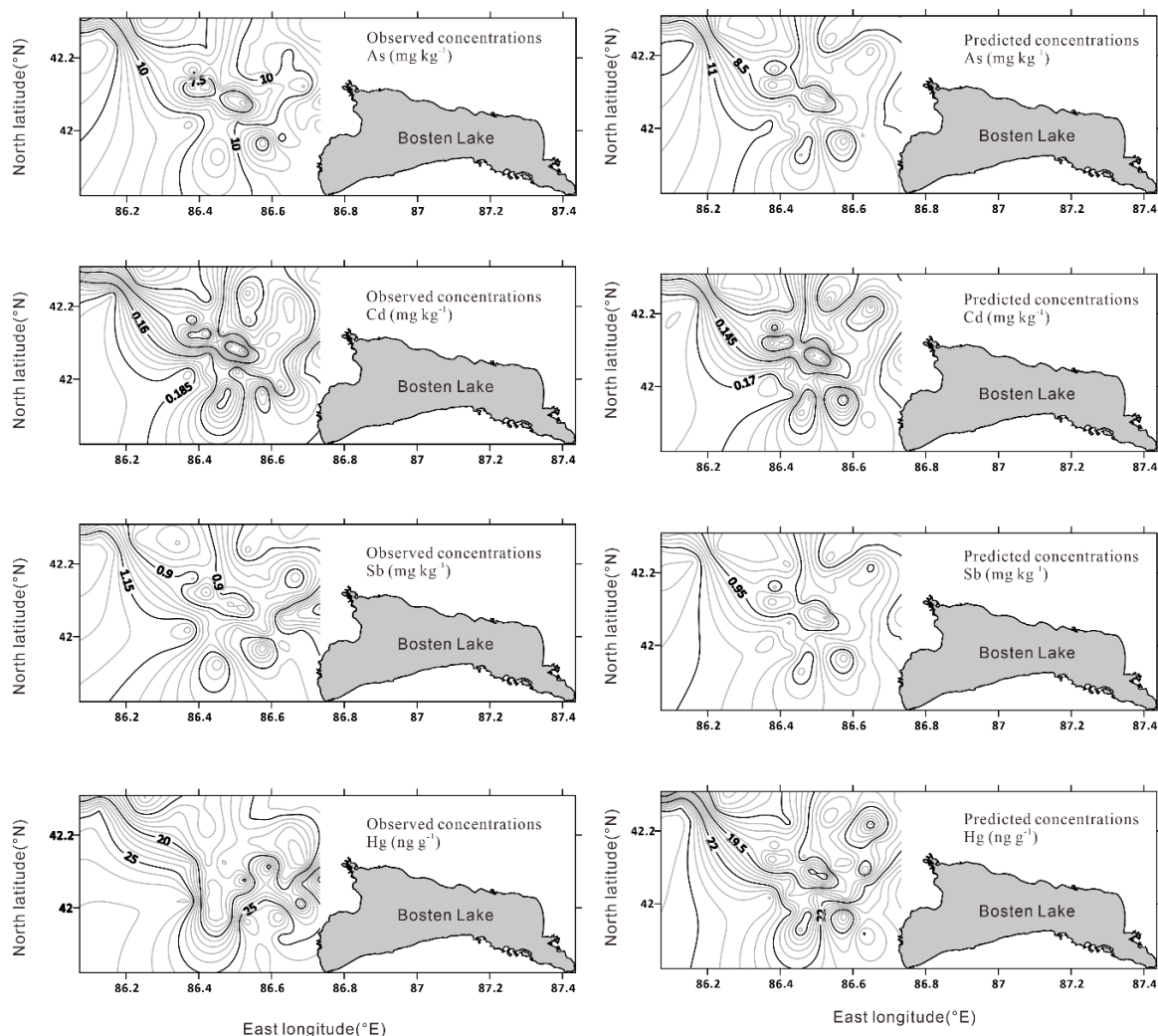


**Figure 4.** Geographically weighted regression predicted concentrations of potentially toxic elements compared with the observed/measured values in the Bosten Lake region.

Simply comparing the difference in heavy metal content between the study region and other regions has no practical significance. By calculating the health risks associated with potentially toxic elements, the extent of contamination in different regions can be reflected to some extent. Based on the risk assessment calculation for heavy metal pollution, the hazard quotient (HQ) via the ingestion ( $HQ_{ing}$ ) of surface soils are higher than those via inhalation ( $HQ_{inh}$ ) and dermal absorption ( $HQ_{dermal}$ ) (Table 3). Different from the degree of pollution in other economically developed regions around the world [65], the health risk index value for potentially toxic elements is less than one (Table 3), which is similar to that for the Issyk-Kul basin [66] and a suburban region of Bishkek [28] in the same arid region of Central Asia. Although this result reflects that the concentration of potentially toxic elements in arid areas has not reached a hazardous level, some potentially toxic elements (As, Cd, Sb, and Hg) have been significantly affected by the surface environment and they need to be paid enough attention.



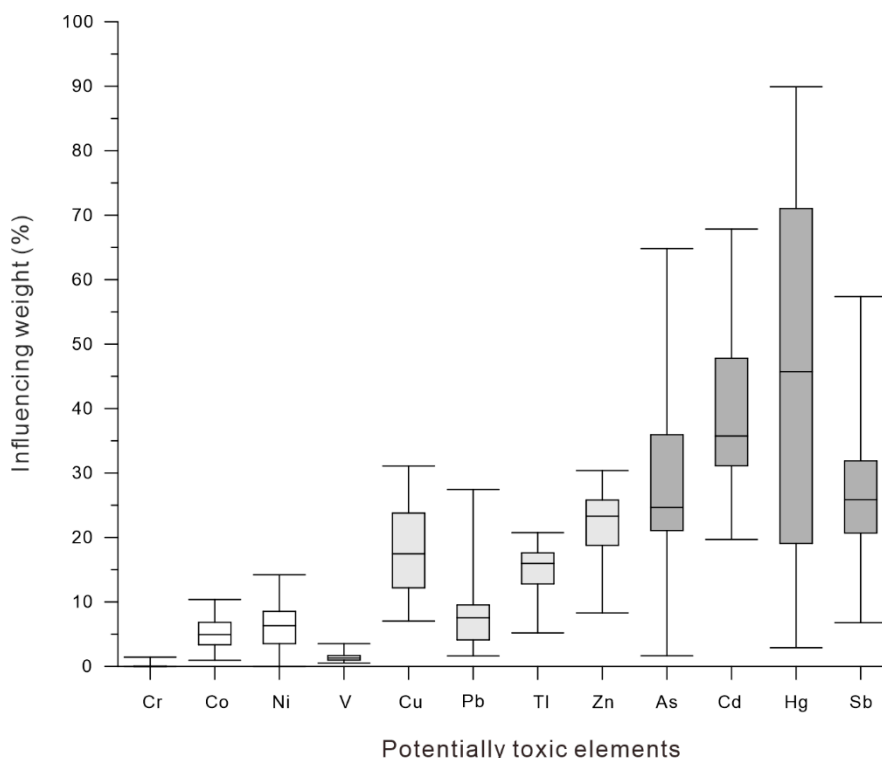


**Figure 5.** Statistical plots indicating the percentage of the potentially toxic elements (Cr, Co, Ni, V, Cu, Pb, Tl, Zn, As, Cd, Hg, and Sb) affected by soil organic matter, which show the minimum, maximum, median, lower quartile, and upper quartile values.

**Table 3.** Human health risk assessment for potentially toxic elements (PTEs) in the surface soils of the Bosten Lake basin.

| PTEs | Maximum                  | Reference Dose for Exposure Pathway (RfD <sub>i</sub> ) [55] (mg kg <sup>-1</sup> day <sup>-1</sup> ) |                         |                         | Non-Carcinogenic Hazards Index |                         |                         |                         |
|------|--------------------------|---|-------------------------|-------------------------|--------------------------------|-------------------------|-------------------------|-------------------------|
|      |                          | RfD <sub>ing</sub>  | RfD <sub>dermal</sub>   | RfD <sub>inh</sub>      | HQ <sub>ing</sub>              | HQ <sub>inh</sub>       | HQ <sub>dermal</sub>    | HI                      |
| V    | 13.7 mg kg <sup>-1</sup> | 7.00 × 10 <sup>-3</sup>   | 7.00 × 10 <sup>-5</sup> | 7.00 × 10 <sup>-3</sup> | 3.69 × 10 <sup>-2</sup>        | 1.73 × 10 <sup>-6</sup> | 1.60 × 10 <sup>-2</sup> | 5.29 × 10 <sup>-2</sup> |
| Zn   | 0.2 mg kg <sup>-1</sup>  | 3.00 × 10 <sup>-1</sup>   | 6.00 × 10 <sup>-2</sup> | 3.00 × 10 <sup>-1</sup> | 0                              | 3.69 × 10 <sup>-8</sup> | 1.70 × 10 <sup>-5</sup> | 8.01 × 10 <sup>-4</sup> |
| Cr   | 1.5 mg kg <sup>-1</sup>  | 3.00 × 10 <sup>-3</sup>   | 6.00 × 10 <sup>-5</sup> | 2.86 × 10 <sup>-5</sup> | 6.76 × 10 <sup>-2</sup>        | 3.34 × 10 <sup>-4</sup> | 1.47 × 10 <sup>-2</sup> | 8.27 × 10 <sup>-2</sup> |
| Co   | 0.6 mg kg <sup>-1</sup>  | 2.00 × 10 <sup>-2</sup>   | 1.60 × 10 <sup>-2</sup> | 5.69 × 10 <sup>-6</sup> | 1.76 × 10 <sup>-3</sup>        | 2.91 × 10 <sup>-4</sup> | 9.56 × 10 <sup>-6</sup> | 2.06 × 10 <sup>-3</sup> |
| Ni   | 21.9 mg kg <sup>-1</sup> | 2.00 × 10 <sup>-2</sup>   | 5.40 × 10 <sup>-3</sup> | 2.00 × 10 <sup>-2</sup> | 4.85 × 10 <sup>-3</sup>        | 2.28 × 10 <sup>-7</sup> | 7.81 × 10 <sup>-5</sup> | 4.93 × 10 <sup>-3</sup> |
| Cu   | 31.0 mg kg <sup>-1</sup> | 4.00 × 10 <sup>-2</sup>   | 1.20 × 10 <sup>-2</sup> | 4.00 × 10 <sup>-2</sup> | 1.98 × 10 <sup>-3</sup>        | 9.33 × 10 <sup>-8</sup> | 2.87 × 10 <sup>-5</sup> | 2.01 × 10 <sup>-3</sup> |
| As   | 23.4 mg kg <sup>-1</sup> | 3.00 × 10 <sup>-4</sup>   | 1.23 × 10 <sup>-4</sup> | 3.00 × 10 <sup>-4</sup> | 1.25 × 10 <sup>-1</sup>        | 5.88 × 10 <sup>-6</sup> | 3.97 × 10 <sup>-2</sup> | 1.65 × 10 <sup>-1</sup> |
| Cd   | 35.5 mg kg <sup>-1</sup> | 1.00 × 10 <sup>-3</sup>   | 1.00 × 10 <sup>-5</sup> | 1.00 × 10 <sup>-3</sup> | 5.50 × 10 <sup>-4</sup>        | 2.59 × 10 <sup>-8</sup> | 2.39 × 10 <sup>-4</sup> | 7.89 × 10 <sup>-4</sup> |
| Sb   | 94.2 mg kg <sup>-1</sup> | 4.00 × 10 <sup>-4</sup>   | 8.00 × 10 <sup>-6</sup> | 4.01 × 10 <sup>-4</sup> | 1.01 × 10 <sup>-2</sup>        | 4.73 × 10 <sup>-7</sup> | 2.19 × 10 <sup>-3</sup> | 1.22 × 10 <sup>-2</sup> |
| Tl   | 85.8 mg kg <sup>-1</sup> | 8.00 × 10 <sup>-5</sup>   | 1.00 × 10 <sup>-5</sup> | 8.00 × 10 <sup>-5</sup> | 2.00 × 10 <sup>-2</sup>        | 9.42 × 10 <sup>-7</sup> | 6.96 × 10 <sup>-4</sup> | 2.07 × 10 <sup>-2</sup> |
| Pb   | 74.1 mg kg <sup>-1</sup> | 3.50 × 10 <sup>-3</sup>   | 5.25 × 10 <sup>-4</sup> | 3.51 × 10 <sup>-3</sup> | 1.72 × 10 <sup>-2</sup>        | 8.06 × 10 <sup>-7</sup> | 4.98 × 10 <sup>-4</sup> | 1.77 × 10 <sup>-2</sup> |
| Hg   | 12.8 ng g <sup>-1</sup>  | 3.00 × 10 <sup>-4</sup>   | 2.10 × 10 <sup>-5</sup> | 3.00 × 10 <sup>-4</sup> | 2.83 × 10 <sup>-4</sup>        | 1.33 × 10 <sup>-8</sup> | 1.76 × 10 <sup>-5</sup> | 3.01 × 10 <sup>-4</sup> |

#### 4. Conclusions

Due to the lack of research on potentially toxic elements in soils in the arid region of Central Asia, a comprehensive study was conducted by analyzing Bosten Lake basin soils, and the method of geographically weighted regression provided a quantitative way to reveal possible influencing factors and model the distribution of potentially toxic elements. The detailed conclusions are as follows:

(1) Based on the calculations from the human health risk assessment, HI < 1 suggests that no significant non-carcinogenic risks to human health occurred in this region.

(2) At the basin scale, most potentially toxic elements had significant gradient changes. Potentially toxic elements (As, Cd, Hg, and Sb) were more susceptible to the organic matter in soils.

(3) Compared with the classical linear model, the modeling results were significantly improved with the geographically weighted regression, which suggested that spatial heterogeneity existed in the relationships among the potentially toxic elements and environmental variables.

(4) By calculating the ratio of the part of the potentially toxic elements affected by the organic matter content and that affected by the parent materials, the rates affected by organic matter were 28.8%, 39.2%, 46.5%, and 26.6% for the potentially toxic elements of As, Cd, Hg, and Sb, respectively.

**Supplementary Materials:** The following are available online at <http://www.mdpi.com/1660-4601/16/19/3741/s1>, Table S1: Total variance explained for potentially toxic elements with Principal Component Analysis; Table S2: The detailed parameters for geographically weighted regression in Table 2; Figure S1: Residuals normality test of the residuals for the fitting results of potentially toxic elements (As, Cd, Sb, and Hg) with geographically weighted regression and classical linear model.

**Author Contributions:** Formal analysis, L.M.; funding acquisition, J.A.; investigation, L.M. and W.L.; methodology, L.M. and W.L.; project administration, J.A.; writing—original draft, L.M.

**Funding:** This research is funded by the Strategic Priority Research Program of the Chinese Academy of Sciences (XDA20060303), West Light Foundation of the Chinese Academy of Sciences (2016-QNXZ-A-4), Tianshan Youth Program of Xinjiang Uygur Autonomous Region, China (2018Q008).

**Acknowledgments:** We thank three anonymous reviewers for their helpful comments and suggestions that improved the manuscript. We acknowledge the Strategic Priority Research Program of the Chinese Academy of Sciences, West Light Foundation of the Chinese Academy of Sciences, and Youth Innovation Promotion Association, CAS.

**Conflicts of Interest:** The authors declare no conflict of interest.

## References

1. Vitousek, P.M.; Mooney, H.A.; Lubchenco, J.; Melillo, J.M. Human Domination of Earth's Ecosystems. *Science* **1997**, *277*, 494. [[CrossRef](#)]
2. Crutzen, P.J. The "anthropocene". In *Earth System Science in the Anthropocene*; Springer: Berlin, Germany, 2006; pp. 13–18.
3. Falkowski, P.; Scholes, R.; Boyle, E.; Canadell, J.; Canfield, D.; Elser, J.; Gruber, N.; Hibbard, K.; Högberg, P.; Linder, S. The global carbon cycle: A test of our knowledge of earth as a system. *Science* **2000**, *290*, 291–296. [[CrossRef](#)] [[PubMed](#)]
4. Senesil, G.S.; Baldassarre, G.; Senesi, N.; Radina, B. Trace element inputs into soils by anthropogenic activities and implications for human health. *Chemosphere* **1999**, *39*, 343–377. [[CrossRef](#)]
5. Jia, Z.; Li, S.; Wang, L. Assessment of soil heavy metals for eco-environment and human health in a rapidly urbanization area of the upper Yangtze Basin. *Sci. Rep.* **2018**, *8*, 3256. [[CrossRef](#)] [[PubMed](#)]
6. Sun, Y.; Zhou, Q.; Xie, X.; Liu, R. Spatial, sources and risk assessment of heavy metal contamination of urban soils in typical regions of Shenyang, China. *J. Hazard. Mater.* **2010**, *174*, 455–462. [[CrossRef](#)] [[PubMed](#)]
7. Naccari, C.; Cicero, N.; Ferrantelli, V.; Giangrosso, G.; Vella, A.; Macaluso, A.; Naccari, F.; Dugo, G. Toxic Metals in Pelagic, Benthic and Demersal Fish Species from Mediterranean FAO Zone 37. *Bull. Environ. Contam. Toxicol.* **2015**, *95*, 567–573. [[CrossRef](#)] [[PubMed](#)]
8. Salvo, A.; Cicero, N.; Vadalà, R.; Mottese, A.F.; Bua, D.; Mallamace, D.; Giannetto, C.; Dugo, G. Toxic and essential metals determination in commercial seafood: *Paracentrotus lividus* by ICP-MS. *Nat. Prod. Res.* **2016**, *30*, 657–664. [[CrossRef](#)] [[PubMed](#)]
9. Li, Z.; Ma, Z.; van der Kuijp, T.J.; Yuan, Z.; Huang, L. A review of soil heavy metal pollution from mines in China: Pollution and health risk assessment. *Sci. Total Environ.* **2014**, *468*, 843–853. [[CrossRef](#)]
10. Kumar, V.; Sharma, A.; Kaur, P.; Singh Sidhu, G.P.; Bali, A.S.; Bhardwaj, R.; Thukral, A.K.; Cerda, A. Pollution assessment of heavy metals in soils of India and ecological risk assessment: A state-of-the-art. *Chemosphere* **2019**, *216*, 449–462. [[CrossRef](#)] [[PubMed](#)]
11. Bi, C.; Zhou, Y.; Chen, Z.; Jia, J.; Bao, X. Heavy metals and lead isotopes in soils, road dust and leafy vegetables and health risks via vegetable consumption in the industrial areas of Shanghai, China. *Sci. Total Environ.* **2018**, *619*, 1349–1357. [[CrossRef](#)]

12. Hu, W.; Wang, H.; Dong, L.; Huang, B.; Borggaard, O.K.; Hansen, H.C.B.; He, Y.; Holm, P.E. Source identification of heavy metals in peri-urban agricultural soils of southeast China: An integrated approach. *Environ. Pollut.* **2018**, *237*, 650–661. [[CrossRef](#)] [[PubMed](#)]
13. Turner, A.; Lewis, M. Lead and other heavy metals in soils impacted by exterior legacy paint in residential areas of south west England. *Sci. Total Environ.* **2018**, *619*, 1206–1213. [[CrossRef](#)] [[PubMed](#)]
14. Loska, K.; Wiechuła, D. Application of principal component analysis for the estimation of source of heavy metal contamination in surface sediments from the Rybnik Reservoir. *Chemosphere* **2003**, *51*, 723–733. [[CrossRef](#)]
15. Han, Y.; Du, P.; Cao, J.; Posmentier, E.S. Multivariate analysis of heavy metal contamination in urban dusts of Xi'an, Central China. *Sci. Total Environ.* **2006**, *355*, 176–186. [[CrossRef](#)]
16. Ma, L.; Wu, J.; Abuduwaili, J. Geochemical evidence of the anthropogenic alteration of element composition in lacustrine sediments from Wuliangsu Lake, North China. *Quat. Int.* **2013**, *306*, 107–113. [[CrossRef](#)]
17. Guan, Q.; Wang, F.; Xu, C.; Pan, N.; Lin, J.; Zhao, R.; Yang, Y.; Luo, H. Source apportionment of heavy metals in agricultural soil based on PMF: A case study in Hexi Corridor, Northwest China. *Chemosphere* **2018**, *193*, 189–197. [[CrossRef](#)] [[PubMed](#)]
18. Huang, Y.; Li, T.; Wu, C.; He, Z.; Japenga, J.; Deng, M.; Yang, X. An integrated approach to assess heavy metal source apportionment in peri-urban agricultural soils. *J. Hazard. Mater.* **2015**, *299*, 540–549. [[CrossRef](#)] [[PubMed](#)]
19. Hu, Y.; Cheng, H. Application of Stochastic Models in Identification and Apportionment of Heavy Metal Pollution Sources in the Surface Soils of a Large-Scale Region. *Environ. Sci. Technol.* **2013**, *47*, 3752–3760. [[CrossRef](#)] [[PubMed](#)]
20. Facchinelli, A.; Sacchi, E.; Mallen, L. Multivariate statistical and GIS-based approach to identify heavy metal sources in soils. *Environ. Pollut.* **2001**, *114*, 313–324. [[CrossRef](#)]
21. Lioubimtseva, E.; Cole, R.; Adams, J.M.; Kapustin, G. Impacts of climate and land-cover changes in arid lands of Central Asia. *J. Arid. Environ.* **2005**, *62*, 285–308. [[CrossRef](#)]
22. Chuluun, T.; Ojima, D. Land use change and carbon cycle in arid and semi-arid lands of East and Central Asia. *Sci. China Ser. C* **2002**, *45*, 48–54.
23. Klein, I.; Gessner, U.; Kuenzer, C. Regional land cover mapping and change detection in Central Asia using MODIS time-series. *Appl. Geogr.* **2012**, *35*, 219–234. [[CrossRef](#)]
24. Lal, R. Carbon sequestration in soils of central Asia. *Land Degrad. Dev.* **2004**, *15*, 563–572. [[CrossRef](#)]
25. Funakawa, S.; Kosaki, T. Potential risk of soil salinization in different regions of Central Asia with special reference to salt reserves in deep layers of soils. *Soil Sci. Plant Nut.* **2007**, *53*, 634–649. [[CrossRef](#)]
26. O'Hara, S.L. Irrigation and land degradation: Implications for agriculture in Turkmenistan, Central Asia. *J. Arid Environ.* **1997**, *37*, 165–179. [[CrossRef](#)]
27. Saiko, T.A.; Zonn, I.S. Irrigation expansion and dynamics of desertification in the Circum-Aral region of Central Asia. *Appl. Geogr.* **2000**, *20*, 349–367. [[CrossRef](#)]
28. Ma, L.; Abuduwaili, J.; Li, Y.; Liu, W. Anthropogenically disturbed potentially toxic elements in roadside topsoils of a suburban region of Bishkek, Central Asia. *Soil Use Manag.* **2019**, *35*, 283–292. [[CrossRef](#)]
29. Chen, J.; Chen, F.; Feng, S.; Huang, W.; Liu, J.; Zhou, A. Hydroclimatic changes in China and surroundings during the Medieval Climate Anomaly and Little Ice Age: Spatial patterns and possible mechanisms. *Quat. Sci. Rev.* **2015**, *107*, 98–111. [[CrossRef](#)]
30. He, Y.; Zhao, C.; Song, M.; Liu, W.; Chen, F.; Zhang, D.; Liu, Z. Onset of frequent dust storms in northern China at ~AD 1100. *Sci. Rep.* **2015**, *5*, 17111. [[CrossRef](#)]
31. Xu, J.; Guo, J.-Y.; Liu, G.-R.; Shi, G.-L.; Guo, C.-S.; Zhang, Y.; Feng, Y.-C. Historical trends of concentrations, source contributions and toxicities for PAHs in dated sediment cores from five lakes in western China. *Sci. Total Environ.* **2014**, *470*, 519–526. [[CrossRef](#)]
32. Guo, J.; Wu, F.; Luo, X.; Liang, Z.; Liao, H.; Zhang, R.; Li, W.; Zhao, X.; Chen, S.; Mai, B. Anthropogenic input of polycyclic aromatic hydrocarbons into five lakes in Western China. *Environ. Pollut.* **2010**, *158*, 2175–2180. [[CrossRef](#)] [[PubMed](#)]
33. Liu, Y.; Mu, S.; Bao, A.; Zhang, D.; Pan, X. Effects of salinity and (an) ions on arsenic behavior in sediment of Bosten Lake, Northwest China. *Environ. Earth Sci.* **2015**, *73*, 4707–4716. [[CrossRef](#)]

34. Guo, W.; Huo, S.; Xi, B.; Zhang, J.; Wu, F. Heavy metal contamination in sediments from typical lakes in the five geographic regions of China: Distribution, bioavailability, and risk. *Ecol. Eng.* **2015**, *81*, 243–255. [[CrossRef](#)]
35. Shen, B.; Jinglu, W.U.; Zhao, Z. Organochlorine pesticides and polycyclic aromatic hydrocarbons in water and sediment of the Bosten Lake, Northwest China. *J. Arid Land* **2017**, *9*, 287–298. [[CrossRef](#)]
36. Wheeler, D.C. Geographically Weighted Regression. In *Handbook of Regional Science*; Fischer, M.M., Nijkamp, P., Eds.; Springer: Berlin, Germany, 2014; pp. 1435–1459.
37. Xia, F.; Qu, L.; Wang, T.; Luo, L.; Chen, H.; Dahlgren, R.A.; Zhang, M.; Mei, K.; Huang, H. Distribution and source analysis of heavy metal pollutants in sediments of a rapid developing urban river system. *Chemosphere* **2018**, *207*, 218–228. [[CrossRef](#)] [[PubMed](#)]
38. Wu, S.-S.; Yang, H.; Guo, F.; Han, R.-M. Spatial patterns and origins of heavy metals in Sheyang River catchment in Jiangsu, China based on geographically weighted regression. *Sci. Total Environ.* **2017**, *580*, 1518–1529. [[CrossRef](#)]
39. Yu, W.; Liu, Y.; Ma, Z.; Bi, J. Improving satellite-based PM 2.5 estimates in China using Gaussian processes modeling in a Bayesian hierarchical setting. *Sci. Rep.* **2017**, *7*, 7048. [[CrossRef](#)]
40. Chen, F.; Huang, X.; Zhang, J.; Holmes, J.A.; Chen, J. Humid Little Ice Age in arid central Asia documented by Bosten Lake, Xinjiang, China. *Sci. China Ser. D* **2006**, *49*, 1280–1290. [[CrossRef](#)]
41. Zhang, J.; Zhou, C.; Li, J. Spatial pattern and evolution of oases in the Yanqi Basin, Xinjiang. *Geogr. Res.* **2006**, *25*, 350–358. [[CrossRef](#)]
42. Wünnemann, B.; Mischke, S.; Chen, F. A Holocene sedimentary record from Bosten Lake, China. *Palaeogeogr. Palaeoclimatol. Palaeoecol.* **2006**, *234*, 223–238. [[CrossRef](#)]
43. Guo, M.; Wu, W.; Zhou, X.; Chen, Y.; Li, J. Investigation of the dramatic changes in lake level of the Bosten Lake in northwestern China. *Theor. Appl. Climatol.* **2015**, *119*, 341–351. [[CrossRef](#)]
44. Zhou, H.; Chen, Y.; Perry, L.; Li, W. Implications of climate change for water management of an arid inland lake in Northwest China. *Lake Reserv. Manag.* **2015**, *31*, 202–213. [[CrossRef](#)]
45. Wang, S.; Radny, D.; Huang, S.; Zhuang, L.; Zhao, S.; Berg, M.; Jetten, M.S.M.; Zhu, G. Nitrogen loss by anaerobic ammonium oxidation in unconfined aquifer soils. *Sci. Rep.* **2017**, *7*, 40173. [[CrossRef](#)] [[PubMed](#)]
46. Chabukdhara, M.; Nema, A.K. Assessment of heavy metal contamination in Hindon River sediments: A chemometric and geochemical approach. *Chemosphere* **2012**, *87*, 945–953. [[CrossRef](#)] [[PubMed](#)]
47. Xu, X.; Zhao, Y.; Zhao, X.; Wang, Y.; Deng, W. Sources of heavy metal pollution in agricultural soils of a rapidly industrializing area in the Yangtze Delta of China. *Ecotox. Environ. Saf.* **2014**, *108*, 161–167. [[CrossRef](#)] [[PubMed](#)]
48. Franco-Uría, A.; López-Mateo, C.; Roca, E.; Fernández-Marcos, M.L. Source identification of heavy metals in pastureland by multivariate analysis in NW Spain. *J. Hazard. Mater.* **2009**, *165*, 1008–1015. [[CrossRef](#)]
49. Hou, D.; O'Connor, D.; Nathanail, P.; Tian, L.; Ma, Y. Integrated GIS and multivariate statistical analysis for regional scale assessment of heavy metal soil contamination: A critical review. *Environ. Pollut.* **2017**, *231*, 1188–1200. [[CrossRef](#)]
50. Grégoire, G. Multiple Linear Regression. *Eur. Astron. Soc. Publ. Ser.* **2014**, *66*, 45–72. [[CrossRef](#)]
51. Fotheringham, A.S.; Charlton, M.E.; Brunson, C. Spatial variations in school performance: A local analysis using geographically weighted regression. *Geogr. Environ. Model.* **2001**, *5*, 43–66. [[CrossRef](#)]
52. Tu, J.; Xia, Z.-G. Examining spatially varying relationships between land use and water quality using geographically weighted regression I: Model design and evaluation. *Sci. Total Environ.* **2008**, *407*, 358–378. [[CrossRef](#)]
53. Nakaya, T. GWR4 User Manual. Available online: [http://www.st-andrews.ac.uk/geoinformatics/wp-content/uploads/GWR4manual\\_201311.pdf](http://www.st-andrews.ac.uk/geoinformatics/wp-content/uploads/GWR4manual_201311.pdf) (accessed on 4 November 2013).
54. Moriasi, D.N.; Arnold, J.G.; Van Liew, M.W.; Bingner, R.L.; Harmel, R.D.; Veith, T.L. Model evaluation guidelines for systematic quantification of accuracy in watershed simulations. *Trans. ASABE* **2007**, *50*, 885–900. [[CrossRef](#)]
55. Ferreira-Baptista, L.; De Miguel, E. Geochemistry and risk assessment of street dust in Luanda, Angola: A tropical urban environment. *Atmos. Environ.* **2005**, *39*, 4501–4512. [[CrossRef](#)]
56. Gu, Y.-G.; Gao, Y.-P.; Lin, Q. Contamination, bioaccessibility and human health risk of heavy metals in exposed-lawn soils from 28 urban parks in southern China's largest city, Guangzhou. *Appl. Geochem.* **2016**, *67*, 52–58. [[CrossRef](#)]

57. Qing, X.; Yutong, Z.; Shenggao, L. Assessment of heavy metal pollution and human health risk in urban soils of steel industrial city (Anshan), Liaoning, Northeast China. *Ecotox. Environ. Safe* **2015**, *120*, 377–385. [[CrossRef](#)] [[PubMed](#)]
58. Lu, X.; Zhang, X.; Li, L.Y.; Chen, H. Assessment of metals pollution and health risk in dust from nursery schools in Xi'an, China. *Environ. Res.* **2014**, *128*, 27–34. [[CrossRef](#)] [[PubMed](#)]
59. Chakraborty, S.; Bhattacharya, T.; Singh, G.; Maity, J.P. Benthic macroalgae as biological indicators of heavy metal pollution in the marine environments: A biomonitoring approach for pollution assessment. *Ecotox. Environ. Safe* **2014**, *100*, 61–68. [[CrossRef](#)] [[PubMed](#)]
60. Zahra, A.; Hashmi, M.Z.; Malik, R.N.; Ahmed, Z. Enrichment and geo-accumulation of heavy metals and risk assessment of sediments of the Kurang Nallah—Feeding tributary of the Rawal Lake Reservoir, Pakistan. *Sci. Total Environ.* **2014**, *470*, 925–933. [[CrossRef](#)] [[PubMed](#)]
61. Wu, S.; Zhou, S.; Li, X. Determining the anthropogenic contribution of heavy metal accumulations around a typical industrial town: Xushe, China. *J. Geochem. Explor.* **2011**, *110*, 92–97. [[CrossRef](#)]
62. Nicholson, F.A.; Smith, S.R.; Alloway, B.J.; Carlton-Smith, C.; Chambers, B.J. An inventory of heavy metals inputs to agricultural soils in England and Wales. *Sci. Total Environ.* **2003**, *311*, 205–219. [[CrossRef](#)]
63. Atafar, Z.; Mesdaghinia, A.; Nouri, J.; Homaei, M.; Yunesian, M.; Ahmadimoghaddam, M.; Mahvi, A.H. Effect of fertilizer application on soil heavy metal concentration. *Environ. Monit. Assess.* **2008**, *160*, 83. [[CrossRef](#)] [[PubMed](#)]
64. Nagajyoti, P.C.; Lee, K.D.; Sreekanth, T.V.M. Heavy metals, occurrence and toxicity for plants: A review. *Environ. Chem. Lett.* **2010**, *8*, 199–216. [[CrossRef](#)]
65. Chen, H.; Teng, Y.; Lu, S.; Wang, Y.; Wang, J. Contamination features and health risk of soil heavy metals in China. *Sci. Total Environ.* **2015**, *512*, 143–153. [[CrossRef](#)] [[PubMed](#)]
66. Ma, L.; Abuduwaili, J.; Li, Y.; Ge, Y. Controlling Factors and Pollution Assessment of Potentially Toxic Elements in Topsoils of the Issyk-Kul Lake Region, Central Asia. *Soil. Sediment. Contam.* **2018**, *27*, 147–160. [[CrossRef](#)]



© 2019 by the authors. Licensee MDPI, Basel, Switzerland. This article is an open access article distributed under the terms and conditions of the Creative Commons Attribution (CC BY) license (<http://creativecommons.org/licenses/by/4.0/>).